

## 26th ITTC Parametric Roll Benchmark Study

Arthur M. Reed

*David Taylor Model Basin (NSWC/CD)*

### ABSTRACT

The 26th ITTC Specialist Committee on Stability in Waves was assigned the task of conducting a benchmark of numerical simulation methods for the prediction of the parametric rolling of ships in head seas. The vessel chosen for the benchmark and the organizations which participated in the benchmark and their simulation tools are described. The results of the benchmark are presented.

### KEYWORDS

Parametric roll; Benchmark calculations; Statistical comparisons

### INTRODUCTION

The ITTC Stability in Waves Committee was assigned the task of conducting a benchmark of numerical simulation methods for the prediction of the parametric rolling of ships in head seas. Participants in the study were to be qualified organizations from both inside and outside the ITTC.

This study aimed to evaluate numerical simulation methods currently employed for the prediction of the parametric rolling of ships in waves, and to assess the current level of accuracy of the relevant numerical prediction methods and computer codes by comparison with model-experimental data.

This study was designed to capture the capabilities of the benchmarked numerical methods for ship responses in realistic random sea conditions. The performance of the methods for the selected loading and wave conditions was assessed in comparison to relevant experimental data as well as with respect to the relative performance of each participating method.

The study comprised the simulation of the behavior of a containership in three steepnesses of longitudinal head waves at one ship loading condition. For the selected conditions, the excitation of roll motion is expected as a result of parametric resonance. The simulated motions in six degrees-of-freedom (6-DoF) were to be

recorded and submitted for review to the study coordinator.

### THE SHIP MODEL

The vessel chosen for the study was a model of a C11 class container ship, MARIN Model 8004-2 (Levadou & van 't Veer, 2006; Paulling, 2007; MARIN, 2005, 2009). MARIN provided the hull definition for the study, which was supplied to the benchmark participants in 3 formats. The fully appended hull was tested, with propeller and rudder. The ship was free to move in 6-DoF—surge, sway, heave, roll, pitch and yaw. Thus, the ability of the simulation to maintain course and heading was a part of the benchmark.

The model is a 55th-scale model of a notional 262 m container ship. Its full-scale principal dimensions and mass properties are provided in Table 1. Figure 1 provides the plan view, profile and body plan of the vessel. Figure 2 provides a photograph of the overall model, including the modeling of containers on deck.

The container ship is fitted with a single horn-type rudder and a single 5-bladed propeller. Figure 3 provides a photograph of the stern configuration, including propeller and rudder.

The actual propeller used on the model was a Wageningen B-Series 5.59 propeller. Its characteristics were provided to the participants both graphically and as a table.

The ship model was fitted with bilge keels that were aligned with the streamlines on the hull. Participants were provided with a table providing the gross parameters of the bilge keels, and a drawing of the bilge keels with an embedded table that provided their placement along the girth of the hull. The bilge keels can be seen in Figs. 1 and 2.

**Table 1—Main Particulars and Mass Properties of the Vessel**

Designation	Symbol	Magnitude
<i>Main particulars</i>		
Length between perpendiculars	$L_{PP}$	262.0 m
Breadth	B	40.0 m
Depth	D	24.45 m
Draft molded on FP	$T_F$	11.719 m
Draft molded on AP	$T_A$	12.856 m
Displacement weight	$\Delta$	76020 t
Centre of gravity fwd of station 0	LCG	122.78 m
Centre of gravity above keel	KG	18.40 m
Transverse metacentric height	$GM_T$	2.075 m
Transverse radius of gyration in air	$k_{XX}$	16.73 m
Longitudinal radius of gyration in air	$K_{YY}$	62.55 m
Natural roll period	$T_\phi$	25.2 s

The model was fitted with a simple PID autopilot that operated based on the model's yaw, yaw rate, and sway. Although it is not traditional to most autopilots, the sway component was used to keep the model located in the middle of the basin during the runs.

### PARAMETRIC ROLL BENCHMARK CASES

The parametric roll benchmark experiments comprised of two parts. The first was a set of roll decay tests in calm water at zero speed and at 5 kt, the speed of the parametric roll experiments. The second component was three parametric roll runs at 5 kt in random seas of differing significant wave height for the same wave modal period.

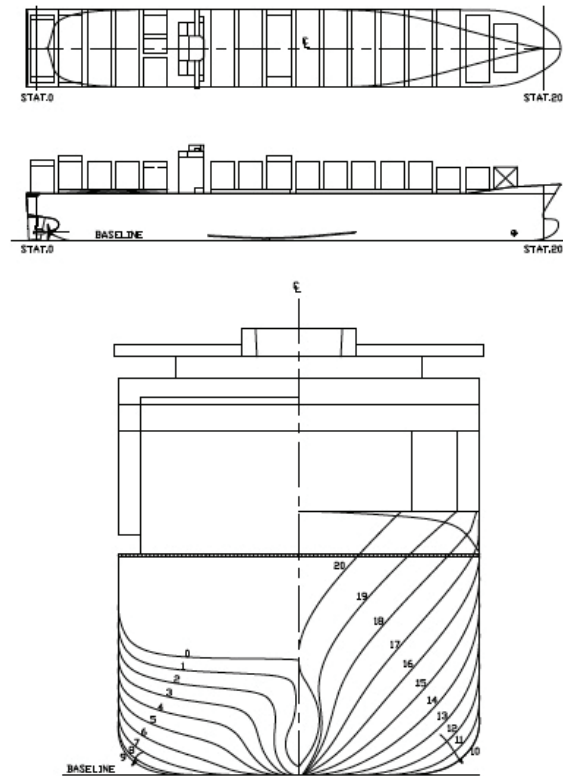


**Fig. 1—General Arrangement and Small Scale Body Plan for MARIN Model 8004-2 (MARIN, 2009).**



**Fig. 2—Side View of MARIN Model 8004-2 (MARIN, 2009).**



**Fig. 3—Stern-Quartering View of MARIN Model 8004-2 Showing Rudder and Propeller (MARIN, 2009).**

The conditions for the three parametric roll runs that are being benchmarked are provided in Table 2. They are all head seas runs at a nominal speed of 5 kt, in spectra with the same modal period but with different significant wave heights.

The wave spectra with phase information that could be used to reconstruct the wave train time histories were provided for the three runs were provided, as were time histories of the actual encountered heights for each run. These wave heights were measured nominally 349 m (full scale) forward of station 10 on the centerline (nominally in the sense that the distance is correct on the average, because the surge motion of the model is not taken into account).

**Table 2—Tests in Irregular Head Seas**

MARIN test no.	Wave conditions	
	Significant wave height [m]	Peak period [s]
307001	4.125	14.4
307002	3.5	14.4
307004	5.25	14.4

For the parametric roll runs, the model was positioned approximately 8.25 full-scale km (150 m model scale) from the wave maker and the wave maker was started. When the waves reached the model, the model and carriage were brought up to speed, and the model proceeded along the tank under the control of the autopilot; tracked by the carriage. Data collection commenced once the model had reached speed.

During all tests, the model was self-propelled at a propeller RPM that was the equivalent of 5 kt full scale in calm water. (The resistance curve, required for the simulations of these cases, was provided to the participants.) Connections between model and carriage consisted only of free-hanging wires for relay of measurement signals and to supply power. These cables did not restrict the motions of the model significantly.

MARIN's Basic Measurement System (BMS) was used for the data acquisition, with a sample rate of 100 Hz, model scale.

Figures 4–9 show the encountered wave and roll time histories for Runs 307001, 307002 and 307004. As can be seen from these figures, the wave elevation time histories increase moderately from Run 307002 to Run 307001 to Run 307004. The roll for Run 307002 is negligible; while Runs 307001 and 307004 both show the occurrence of significant parametric roll.

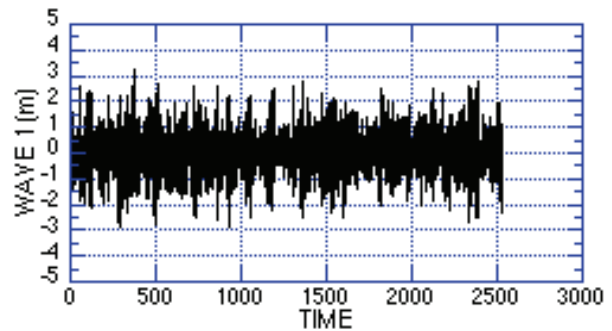


**Fig. 4—Wave time history for MARIN Model 8004-2, Run 307001**

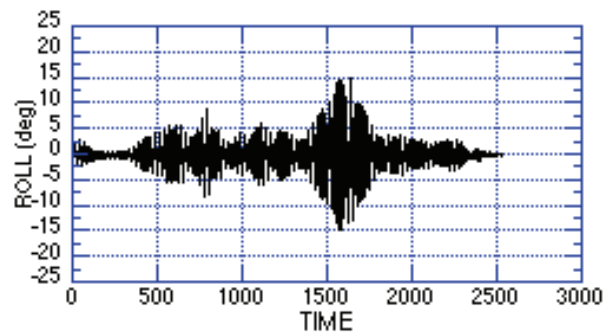


**Fig. 5—Roll time history record for MARIN Model 8004-2, Run 307001**

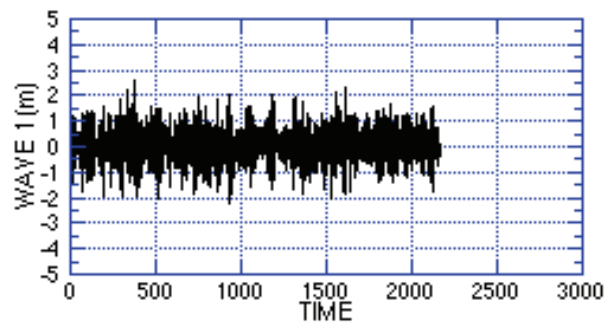


**Fig. 6—Wave time history for MARIN Model 8004-2, Run 307002**

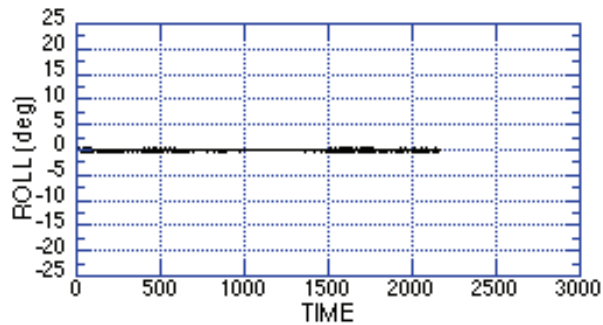


Fig. 7—Roll time history for MARIN Model 8004-2, Run 307002

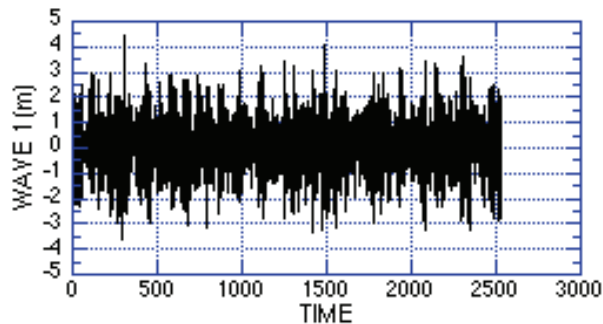


Fig. 8—Wave time history for MARIN Model 8004-2, Run 307004

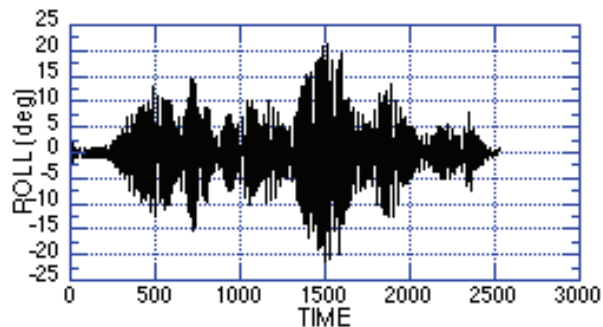


Fig. 9—Roll time history for MARIN Model 8004-2, Run 307004

## BENCHMARK SIMULATIONS

Comparisons of the simulations of parametric roll with the experimental results were to be made based on the statistics of the simulated waves and of the predicted 6-DoF motions; and where possible, on comparisons of the actual 6-DoF motion predictions. For the three cases that were to be compared, participants were asked to perform one set of simulations using the “default” roll damping model from their simulation tool, and if they “tuned” their roll damping against the roll decay data, a second set of simulations using

that tuned roll damping. Additionally, participants were asked to submit their roll decay predictions from their “default” roll decay model and their “tuned” roll decay model.

Initially, ten organizations indicated an interest in participating in the benchmark study, and ultimately, six organizations provided results predicted using seven different computer codes. The six organizations and their computer codes are listed in Table 3.

Brief descriptions of these computational tools are provided below. With the exception of ROLLSS, all of the codes are blended codes that compute the exact nonlinear Froude-Krylov exciting forces due to the incident wave and the exact hydrostatic restoring forces over the instantaneous wetted surface of the vessel, and employ linear computations of the radiation and diffraction forces for the vessel up to the mean waterline. ROLLSS employs a different blending where all forces except for those in roll are calculated linearly. The descriptions, with references, follow:

FREDYN v9.80 and 10.1 (De Kat & Paulling, 2001; Hooft, 1987) simulates the dynamic behaviour of a steered ship subjected to waves and wind. All six degrees of freedom are computed in the time domain, where the motions can be large up to the point of capsize. Nonlinearities arise from rigid-body dynamics with large angles and fluid flow effects. A linear strip theory approach is used to compute the hydrodynamic forces acting on the hull.

ROLLSS (Söding, 1982; Kröger, 1986; Petey 1988, Brunswig, *et al.*, 2006) is a code for the simulation of parametric rolling. While the pitch, heave, sway and yaw motions are computed by a linear strip method, and the surge motion by a simple nonlinear approach, the roll motion is computed nonlinearly in time domain using the righting arm curves for static stability in waves.

OU-PR (Osaka University simulation program for Parametric Rolling) (Hashimoto & Umeda, 2010; Hashimoto, *et al.*, 2011) is a time domain simulation program for prediction parametric rolling in regular and long-crested irregular waves, which uses a 3-DoF coupled of heave-roll-pitch model. The 2-D radiation and diffraction hydrodynamic forces are calculated for the submerged hull with the instantaneous roll angle taken into account. The roll radiation force

is calculated at the natural roll frequency and those in vertical modes (heave and pitch) are at the peak of the mean wave frequency.

Linear and quadratic roll damping is determined from results of a roll decay test if available. Otherwise, they are determined by Ikeda’s semi-empirical method.

**Table 3—Organizations Participating in the Benchmark Study and Their Respective Computer Codes**

Organisation	Code(s)
David Taylor Model Basin (NSWC/CD)	FREDYN, v9.8
HSVA	ROLLSS
MARIN	FREDYN, v10.1
Osaka University	OU-PR
Science Applications International Corporation	LAMP 3
Seoul National University	SNU-PARAROLL, WISH

LAMP 3 (Lin & Yue ,1990; Shin, *et al.*, 2003; Lin, *et al.*, 2006; Yen, *et al.*, 2008, 2010) predicts the motions and loads of a ship operating in a seaway. In LAMP’s simulations, the wave-body hydrodynamic forces are calculated using a 3-D Rankine potential flow panel method with a linearized free-surface boundary condition to solve the wave-body interaction problem in the time domain, while forces due to viscous flow and other “external” effects such as hull lift, propulsors, rudders, *etc.* are modeled using other computation methods, or with empirical or semi-empirical formulas. LAMP’s calculations include 2nd and higher order “drift” forces in the horizontal plane (Zhang, *et al.*, 2009). These drift forces play an important role in the horizontal-plane motions for the prediction of course keeping in waves.

SNU-PARAROLL (Kim & Kim, 2010b; Kim & Kim, 2011) employs a linear impulse-response-function approach to compute the radiation and diffraction forces. The impulse response function approach is basically the conversion of the frequency-domain strip-theory solution into the time domain. In this method, the conversion is limited to the radiation force. The excitation force

includes the nonlinear Froude-Krylov and restoring force and moment on the instantaneous wetted surface as well as the linear diffraction force. The wetted surface is defined as the hull surface wetted by the body motion and the incident wave.

WISH (computer program for nonlinear Wave-Induced loads and SHip motion) (Kim, *et al.*, 2009; Kim & Kim, 2010a,b) is a three-dimensional Rankine panel method used to study nonlinear roll motions. In this method, the total velocity potential is decomposed into three components: the basis flow; the incident wave; and disturbance velocity potentials. In this weakly-nonlinear approach, the disturbed component of the wave and velocity potentials are assumed to be small. The kinematic, dynamic free surface and body boundary conditions are linearized. The basis flow-wave induced motion terms (*m*-terms) are hard to compute, since they require second-order differentials of the basis flow. In this code, the second-order differentials are converted to first-order differentials using Stoke’s theorem.

## BENCHMARK COMPARISONS

### *Statistical Methodology*

The motions that have no restoring force (surge, sway, and yaw) can be significantly affected by the actions of the autopilot and the propulsion algorithm. Taking advantage of the fact that these effects will, in general, be at much lower frequency than the wave encounter frequency, the surge sway and yaw motions are decomposed into “low-frequency” and “wave-frequency” components, to separate the maneuvering and autopilot related contribution to the motions from the direct response to the wave excitation.

The analysis of the results consisted of statistical analysis of the wave elevation and the 6-degree-of-freedom motions. The statistical quantities that are computed are given below:

1. *Mean value:*  $\bar{u}$  (MEAN)

$$\bar{u} = \frac{1}{N} \sum_{n=1}^N u_n \tag{1}$$

where  $u_n$  is the  $n$ -th sample of the signal and  $N$  is number of samples.

2. *Variance of the Mean*:  $V_M$  (VAR MEAN),

$$V_M = V \frac{1}{N} \sum_{i=-N+1}^{N-1} \left(1 - \frac{|i|}{N}\right) \bar{R}_{|i|}, \quad (2)$$

where  $\bar{R}_i$  is the  $i$ -th value of the normalized autocorrelation function of the signal and is the variance of the signal.

3. *Variance*:  $V (= \kappa^2)$  (VAR),

$$V = \frac{1}{N} \sum_{n=1}^N (u_n - \bar{u})^2 \quad (3)$$

4. *Variance of the Variance*:  $V_V$  (VAR VAR),

$$V_V = V^2 \frac{2}{N} \sum_{i=-N+1}^{N-1} \left(1 - \frac{|i|}{N}\right) \bar{R}_{|i|}^2, \quad (4)$$

used to compute a confidence interval for the value of the variance.

Based on the ideas and method of Belenky, *et al.* (2007), the computation of the variance of the mean ( $V_M$ ) and the variance of the variance ( $V_V$ ) allows the computation of confidence bounds for the mean and variance of the experiments and computations. The computation of  $V_M$  and  $V_V$  requires the normalized autocorrelation function  $\bar{R}(t)$  of the measured or computed response.

The normalized autocorrelation function can be computed directly from the signal or from the spectrum of the signal. If  $\bar{R}(t)$  is computed directly from the signal,  $\bar{R}(t)$  must be truncated due to the loss of statistical confidence in the function's values for large lags. The computation of  $\bar{R}(t)$  from the spectrum requires that the spectrum be smoothed before  $\bar{R}(t)$  is computed.

The recommended method for computing  $\bar{R}(t)$  is from the spectrum. The autocorrelation function is the cosine transform of the spectrum, so it can be computed as follows:

$$R(t) = \int_0^{\infty} d\omega S(\omega) \cos \omega t \quad (5)$$

The normalized autocorrelation function  $\bar{R}(t)$  is produced by dividing the autocorrelation function  $\bar{R}(t)$  by the approximate variance  $V' [= R(0)]$ , so that  $\bar{R}(0)$  is identically 1.

$$\bar{R}(t) = \frac{1}{V'} R(t) = \frac{1}{R(0)} R(t). \quad (6)$$

This normalization is required to account for the computational and/or truncation errors that are likely to accrue in the computation of the spectrum and the autocorrelation function from the spectrum, which result in a difference between the approximate variance  $V' [= R(0)]$  and the true variance of the signal,  $V$ .

The spectrum of the encountered wave train, complete motions (heave, roll, and pitch) and wave-frequency decomposed motions (surge, sway, and yaw) are computed in the usual manner using Fourier transforms. As seen in Figure 10, this spectrum will be quite jagged; and the normalized autocorrelation function computed from this jagged spectrum will not continuously decrease for large lag times, Figure 11.

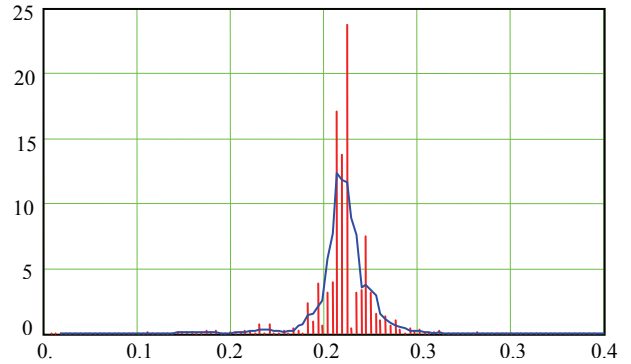


Fig. 10—Raw Roll Spectrum and Roll Spectrum Smoothed with 5-Point Boxcar Filter.

Smoothing the spectrum before computing the normalized autocorrelation function improves the quality of  $R(t)$  and reduces the growth of the envelope for large lag times. The smoothing can be performed by using a digital filter, or more easily by means of a “boxcar” filter, a simple 5-point running average filter that sets the new value of point  $n$  to be the average of the 5 points centered about point  $n$ . The spectrum smoothed with a 5-point boxcar filter is shown in Figure 10 and the resulting normalized autocorrelation function is given in Figure 12. A boxcar filter with more points (7, 9 or 11) produces a smoother spectrum and better looking autocorrelation function, but has little effect on the computed values of  $V_M$  and  $V_V$ .

Once the normalized autocorrelation function has been computed, it is straightforward to

compute the variance of the mean,  $V_M$  and variance of the variance  $V_V$  of the measured or computed signal, using equations (2) and (4), respectively.

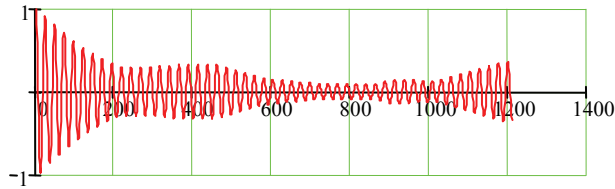


Fig. 11—Normalized Roll Autocorrelation Function from Raw Spectrum.

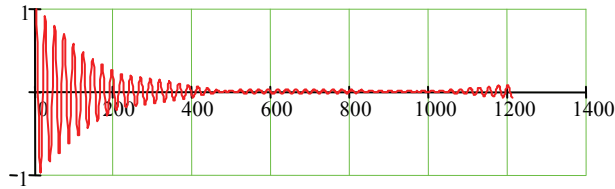


Fig. 12—Normalized Roll Autocorrelation Function from Spectrum Smoothed with 5-Point Boxcar Filter.

### Comparisons

Although all participants provided the statistics for the waves and all 6-DoF of motion, the allotted space does not allow all of the results to be presented. Thus, only the wave and roll statistics are being provided. Figure 13 shows the variance of the wave time histories from the experiments and each of the predictions along with the corresponding 95% confidence bands. Figure 14 shows similar results for roll. On these plots, the experiments are denoted by “Ex” and the predictions have been randomly assigned the letters “A” to “G”.

Examining the variance of the wave height shown in Fig 13, it is seen that the variance of the wave heights are consistent with the experimental results for all three runs. Additionally, all of the predictions are well within the 95% confidence band of the experimental results.

The statistics for roll shown in Figure 14 exhibit much less agreement between the predictions and the experimental results.

For Run 307002, only methods F and G show any notable roll response. None of the experiments or computations except for F and G have any significant variance of the variance.

In the case of Run 307001, the experiments show significant variance and 95% confidence

bands, while methods B, F, and G show significant variance and have significant 95% confidence bands. None of the other methods show either any variance or 95% confidence bands. In fact the upper 95% confidence limits for the predictions by methods A, C, D and E are below the 95% confidence band for the experiments. Methods B, F and G have 95% confidence bands comparable to that of the experiments, which overlap the experimental 95% confidence band—statistically, all of these results are the same.

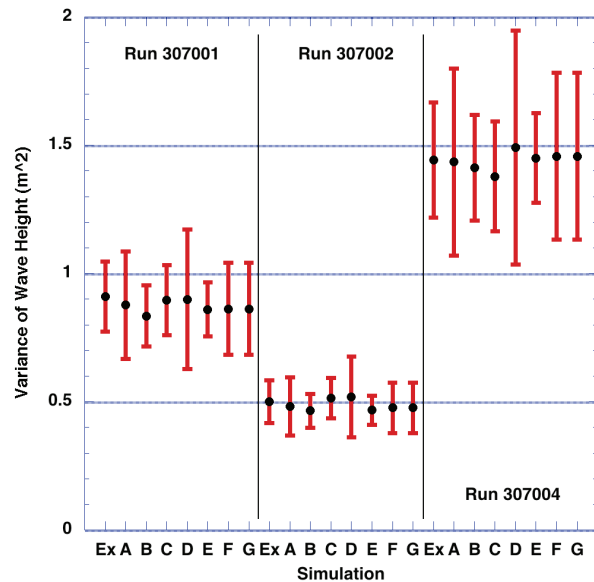


Fig. 13—Variance of wave height with 95% confidence bands for MARIN Model 8004-2, Runs 307001, 307002, and 307004, as predicted from the experiments (Ex) and computations (A–G).

The results for Run 307004 are different from both of the previous runs. The experimental results show a lower 95% confidence limit, which is negative, an impossibility, which indicates that the usual normal distribution assumptions are not applicable. (The same comment applies to Method B in Run 307001 and Methods F and G in Run 307002.) In fact the 95% confidence band limits must be computed assuming a truncated normal distribution, and this will lead to upper and lower limits of 89.5 deg<sup>2</sup> and 2.7 deg<sup>2</sup>, respectively. With the exception of method C the variance of all of the predictions are within the 95% confidence band of the experiments, and are statistically equivalent.

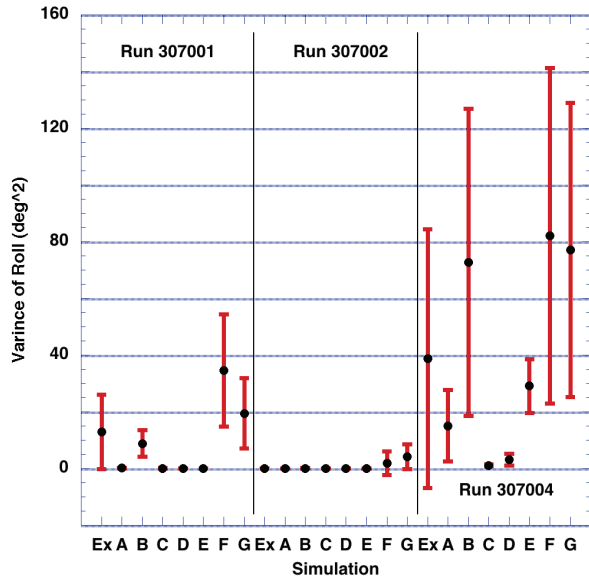


Fig. 14: Variance of roll angle with 95% confidence bands for MARIN Model 8004-2, Runs 307001, 307002, and 307004, as predicted from the experiments (Ex) and computations (A–G).

### BENCHMARK CONCLUSIONS

The results of the SAFEDOR Parametric Roll Benchmark (Spanos & Papanikolaou, 2009a,b) provide no confidence bands, but show levels of scatter in the range of roll predictions consistent with those seen in Figure 14—they have more participating codes and more cases. Thus the scatter in the variance of the predictions should not have been unexpected.

Belenky & Weems (2011) have conducted a study where they used LAMP 2 to predict the head-sea motions of a C11 class container vessel, looking for parametric roll. They produced 50 realizations of the same JONSWAP spectrum, where each realization consisted of 1500 s of data. They then computed the 95% confidence interval for the roll variance for each individual realization and for the ensemble of all 50 realizations. Figure 15 shows the variance of the roll along with the confidence interval for each individual run and for the ensemble of 50 runs.

Figure 15 shows the degree of variability that can occur from run to run. The variance of the first and second realizations differ by more than a factor of two ( $29 \text{ deg}^2$  vs.  $72 \text{ deg}^2$ ), and the largest and smallest vary by a factor of five ( $15 \text{ deg}^2$  vs.  $77 \text{ deg}^2$ ). As can be seen, the ensemble

confidence band is significantly narrower than those of the individual records.

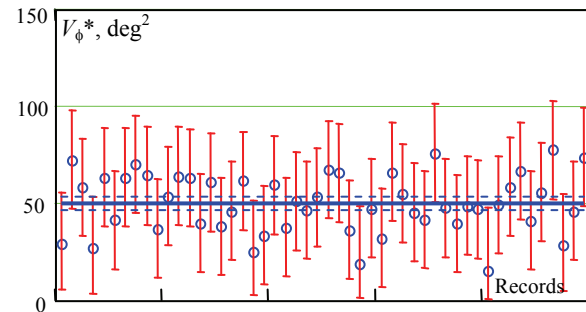


Fig. 15: Estimates of Variance Values of Records and Ensemble (from Belenky & Weems, 2011)

The reason for the dramatic differences in the variance of the records is the fact that parametric roll is a consequence of a group of waves of length close to the ship length and a speed-heading combination that results in an encounter frequency that is twice the roll natural frequency. The practical implications of this are that an individual record contains little statistically independent data. Thus, these waves have a narrow spectral peak that results in an autocorrelation function that does not decay quickly with lag time.

To characterize the solution to this problem, Belenky & Weems go on to study the number of records that must be ensemble averaged in order to produce a “tight” statistical characterization of the variance of the roll. This is demonstrated in Figure 16, where the convergence of the variance of the ensemble and its confidence interval is shown as a function of the number of records included in the ensemble average.

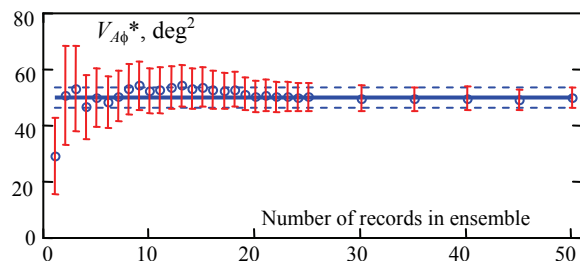


Fig. 16—Convergence of Ensemble Estimate of Variance (from Belenky & Weems, 2011)

As can be seen, after approximately 20 records there is little change in either the variance or the confidence band for the ensemble and, there is significant convergence after as few as 4 or 5

records. Thus, from a practical perspective, as few as 7 to 10 realizations should produce usefully convergent results.

In principle, this problem can be overcome by producing significantly longer records, but this is not in general realistic. It is a manifestation of what Belenky & Weems call practical non-ergodicity, “meaning that several independent records must be used in order to devise any judgment on the statistical characteristics of the parametric roll response.” To characterize the solution to this problem, Belenky & Weems go on to study the number of records that must be ensemble averaged in order to produce a “tight” statistical characterization of the variance of the roll—the convergence of the variance of the ensemble and its confidence interval as a function of the number of records included in the ensemble average. They find that after approximately 20 records there is little change in either the variance or the confidence band for the ensemble and there is significant convergence after as few as 4 or 5 records. Thus, from a practical perspective, as few as 7 to 10 realizations should produce usefully convergent results.

From the perspective of the benchmark study, this indicates that it is not possible to draw any conclusions regarding the performance of any simulation method from a single realization. One may conclude that those methods that have very narrow confidence bands on their results are probably not fully capturing the physics of parametric roll. For either experiments or computations, it will take the results from 7 to 10 realizations at the same significant wave height to determine convergent results. Further, as converged statistical results are obtained, more sophisticated means of comparison than the variance of the roll amplitude, such a roll exceedance rates with the appropriate confidence bands should be used to compare methods.

## REFERENCES

Belenky, V. & K.M. Weems (2011) “Probabilistic Properties of Parametric Roll.” Proc. Workshop on Parametric Resonance in Dynamical Systems, Spitsbergen, Norway, 21 p.

Belenky, V., K.M. Weems & W-M. Lin (2007) “A Probabilistic Procedure for Evaluating the

Dynamic Stability and Capsizing of Naval Vessels, Phase 1: Technology Demonstration.” SAIC Report ASTD 08- 017, 211 p.

Brunswig, J., R. Pereira & D. Kim (2006) “Validation of Parametric Roll Motion Predictions for a Modern Containership Design.” Proc. 9th Int’l Conf. Stability of Ships & Ocean Vehicles, Rio de Janeiro, 14 p.

De Kat, J.O. & J.R. Paulling (2001) “Prediction of extreme motions and capsizing of ships and offshore vehicles.” Proc. 20th Int’l Conf. Offshore Mechanics & Arctic Engin., Rio de Janeiro, 12 p.

Hashimoto H. & N. Umeda (2010) “A study on Quantitative Prediction of Parametric Roll in Regular Waves.” Proc. 11th Intl Ship Stability Workshop, Wageningen, Netherlands, 7 p.

Hashimoto H., N. Umeda & Y. Sogawa (2011) “Prediction of Parametric Rolling in Irregular Head Waves.” Proc. 12th Int’l Ship Stability Workshop, Washington, DC.

Hooft, J.P. (1987) “Mathematical description of the manoeuvrability of high-speed surface ships.” MARIN report No. 47583-1-MO.

Kim, K.H. & Y. Kim (2010a) “Comparative Study on Ship Hydrodynamics Based on Neumann-Kelvin and Double-Body Linearizations in Time-Domain Analysis.” Int’l J. Offshore & Polar Engin., Vol. 20, No 4, pp. 265–274.

Kim, K.H., Y. Kim & M.S. Kim (2009) “Numerical Analysis on Motion Responses of Adjacent Multiple Floating Bodies by Using Rankine Panel Method.” Intl J. Offshore & Polar Engin., Vol 19, No 2.

Kim, T. & Y. Kim (2010b) “Multi-level Approach of Parametric Roll Analysis.” Proc. ITTC Workshop on Seakeeping, Seoul, Korea, 21 p.

Kim, T. & Y. Kim (2011) “Numerical Study on Difference-Frequency-Induced Parametric Roll Occurrence.” Intl J. Offshore & Polar Engin., Vol. 21, No. 1, pp. 1–10.

Kröger, H.P. (1986) “Rollsimulation von Schiffen im Seegang.” Schiffstechnik, Vol. 33

Levadou M. & R. Van’t Veer (2006) “Parametric Roll and Ship Design.” Proc. 9th Int’l Conf. Stability of

- Ships & Ocean Vehicles, Rio de Janeiro, Brazil.
- Lin, W.M. & D.K.P. Yue (1990) "Numerical Solutions for Large-Amplitude Ship Motions in the Time-Domain." Proc. 18th Symp. Naval Hydro., Ann Arbor, MI, pp. 41–66.
- Lin, W.M., S. Zhang, K. Weems & D. Liut (2006) "Numerical Simulations of Ship Maneuvering in Waves." Proc. 26th Symp. Naval Hydro., Rome, Italy.
- MARIN (2005) "Parametric Roll Tests On C11 Post PANAMAX Container Vessel." MARIN Report No. 17701-2-SMB, Vol. 1, 28 p.
- MARIN (2009) "Parametric Roll Tests On C11 Post PANAMAX Container Vessel, Data Report." MARIN Report No. 17701-2-SMB, Vol 2, 280 p.
- Paulling, J. R. (2007) "On Parametric Rolling of Ships." Proc. 10th Int'l Symp. Practical Design of Ships & Other Floating Structures, Houston, TX, 9 p.
- Petey, F. (1988) "Ermittlung der Kentersicherheit lecker Schiffe im Seegang aus Bewegungssimulationen." Report Nr. 487, Institut für Schiffbau der Universität Hamburg
- Shin, Y.S., V.L. Belenky, W.M. Lin, K.M. Weems & A.H. Engle (2003) "Nonlinear Time Domain Simulation Technology for Seakeeping and Wave-Load Analysis for Modern Ship Design." Trans. SNAME, Vol. 111, pp. 557–78.
- Söding, H. (1982) "Leckstabilität im Seegang." Report Nr. 429, Institut für Schiffbau der Universität Hamburg
- Spanos, D. & A. Papanikolaou (2009a) "Benchmark Study on Numerical Simulation Methods for the Prediction of Parametric Roll of Ships in Waves." Proc. 10th Int'l Conf. Stability of Ships & Ocean Vehicles, St Petersburg, Russia.
- Spanos D. & A. Papanikolaou (2009b) "SAFE- DOR International Benchmark Study on Numerical Simulation Methods for the Prediction of Parametric Rolling of Ships in Wave." NTUA-SDL Report, Rev. 1.0, 60 p.
- Yen, T.G., D.A. Liut, S. Zhang, W.M. Lin, & K.M. Weems (2008) "LAMP Simulation of Calm Water Maneuvers for a U.S. Navy Surface Combatant." Workshop on Verification & Validation of Ship Maneuvering Simulation Methods, Copenhagen.
- Yen, T.G., S. Zhang, K. Weems & W.M. Lin (2010) "Development and Validation of Numerical Simulations for Ship Maneuvering in Calm Water and in Waves." Proc. 28th Symp. Naval Hydro., Pasadena, CA.
- Zhang, S., K.M. Weems & W.M. Lin (2009) "Investigation of the Horizontal Drifting Effects on Ships with Forward Speed." Proc. ASME 28th Int'l Conf. Ocean, Offshore & Arctic Engin., Honolulu, HI.